Reconfigurable intelligent surface design using PIN diodes via rotation technique -Proof of concept

Samara Gharbieh, Raffaele D Errico, Antonio Clemente

Reconfigurable Intelligent Surface Design using PIN Diodes via Rotation Technique – Proof of Concept

Samara Gharbieh, Raffaele D'Errico, Antonio Clemente

CEA-Leti, Univ. Grenoble Alpes, F-38000 Grenoble, France

e-mail: {samara.gharbieh, raffaele.derrico, antonio.clemente }@cea.fr

Abstract— **In this paper, we present the design of a reconfigurable intelligent surface (RIS) operating in the Ka-band (27 – 31GHz). The considered RIS operates in reflection mode; thus, it is a reflectarray antenna. The reflectarray unit cell has a relatively simple structure with four metal layers and two Isola Astra MT77 substrates. In order to achieve the electronic phase control of the unit cell, two p-i-n diodes were integrated on the reflecting patch. The alternation of the diodes states will create a rotation in the current distribution on the top of the reflecting patch, and thus a 1-bit phase shift resolution is obtained. The unit cell performances present 1.5 dB losses over the studied band (14% of relative bandwidth). The phase difference between the two unit cell states is 180° at the central frequency with acceptable phase errors over the frequency band. The designed unit cell is then used in the synthesis of reflectarray antennas. For this purpose, an *in-house* synthesis tool is developed to optimize the reflectarray analytically. Furthermore, an 8×8 elements reflectarray is designed using the aforementioned tool, and its theoretical results are compared to a full-wave simulation.**

*Index Terms—***Reconfigurable intelligent surface, reflectaray, 1-bit phase resolution, electronically beamforming, beam scanning.**

I. Introduction

In the past few years, reconfigurable intelligent surfaces (RIS) gained a lot of interest due to their key role in mobile communication networks. They are designed in order to overcome attenuation by receiving a wave and redirecting it towards a desired direction (see Fig. 1). They are expected to achieve secure, unlimited, and uninterrupted connectivity between several type of equipment (such as mobile phones, machines, vehicles, etc.)[1], [2] . Thus, RIS are essentially the same as the conventional transmitarray (TA) [3] and reflectarray (RA) [4]. In this work, we will focus on the reflecting RIS scenario.

As depicted in Fig. 1, RA consist of a focal source with an arrangement of quasi-periodic elements known as the unit cell. The first step in designing a RA is the design of the unit cell. In order to provide the beam steering and beamforming, active elements are integrated into the unit cell architecture. The most popular devices used for this purpose are varactors [5], MEMS [6], and p-i-n diodes [7], [8]. In [9], a circular patch with a rectangular slot loaded by a p-i-n diode is presented. A 180° phase shift is created in [9] by alternating the state of the diode and tuning the distance between the substrate and the ground plane accordingly. Whereas, in [10], the proposed unit cell consists of a parasitic resonator and a square patch. By turning on the p-i-n diode the length of the
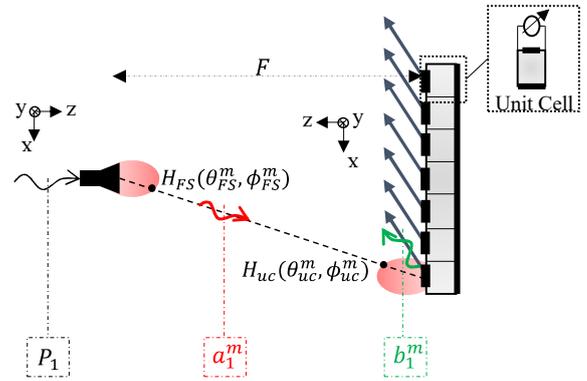

Fig. 1. Operating principle of the RIS in reflecting mode.

resonator in [10] changes, which leads to a shift in the resonance frequency, and therefore a phase difference of 180°.

Several techniques are used to design RA unit cells, for example, varying size patches, varying delay line lengths, and varying rotation angles. To the best of our knowledge, the technique based on varying rotation angles was previously used in the literature only in the case of designing *passive* circularly polarized RA [11]. In our work, we use the aforementioned rotation strategy, to design a 1-bit reconfigurable RA unit cell linearly polarized, where the states of two p-i-n diodes will control the current distribution on top of the patch, and create a 180° phase difference. The proposed unit cell is used to synthesize a RA composed of 8×8 unit cells. The full antenna is optimized using an in-house developed Matlab tool. Furthermore, Full-wave simulations are performed to validate the design and the optimization tool.

The paper is organized as follows. In Section II, we present the unit-cell architecture, its operating principle, and the corresponding simulation results. The RA configuration and modeling tool is shown in Section III.A. The optimized RA illuminated by a 10-dBi horn is presented in Section III.B. The paper is concluded in Section IV with some perspectives for future research.

II. 1-Bit Unit Cell Based On PIN Diodes

A. Geometry of the unit cell and operating principle

The schematic of the proposed linearly-polarized unit-cell is shown in Fig. 2. It is composed of four metal layers printed on two Isola Astra MT77 substrates (ϵ_r= 3, $tan\delta$= 0.0017) and bonded with Astra MT77 pre-preg bonding film (ϵ_r= 2.95, $tan\delta$ = 0.0019). The top layer (Fig. 2 (b)) is the
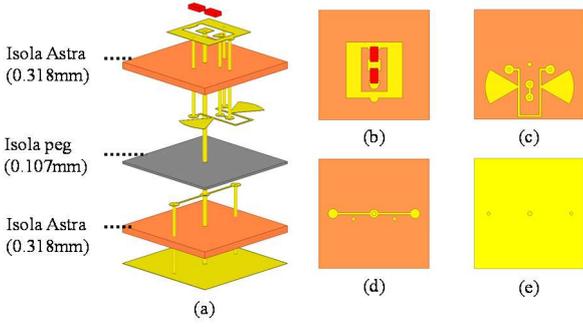
Fig. 2. The proposed 1-bit linearly-polarized unit-cell: (a) Schematic view, (b) radiating element, (c) biasing layer, (d) DC connection to the ground layer, and (e) ground plane.

radiating element. It consists of center-fed O-slot rectangular patch antenna working in reflecting mode. The patch antenna is connected by a metalized via hole located at its center to the ground plane (Fig. 2 (e)). Two p-i-n diodes MA4AGP907 are flip-chipped on the patch antenna to tune the reflection phase, and these diodes are controlled by a bias line (Fig. 2 (c)) printed on the opposite side of the substrate. The bias network includes microstrip radial stubs to isolate the RF signals. The patch is also connected to a delay line (Fig. 2 (c)), printed as well on the opposite side of the substrate. The DC connection to ground is realized with a short circuit stub.

The two p-i-n diodes are biased in opposite states (one p-i-n diode is switched ON while the other one is in OFF state). Due to the presence of the aforementioned delay line (printed in the layer Fig. 2 (c)), a 90° rotation of the current distributions is expected to occur. In the passive case, the rotation of the printed elements in the reflectarray cell by an angle α_{rot} results in a phase shift of $\Delta\phi = 2 \times \alpha_{rot}$ [11]. Therefore, if the alternation states of the diodes will incur a rotation of angle $\alpha_{rot} = 90°$, then a $\Delta\phi = 180°$ phase shift is obtained, i.e., a 1-bit phase quantization.

B. Simulation of the unit cell

The two generated states of the unit cells will be denoted by State000 and State180. As explained in the previous section, and depicted in Fig. 3, the alternation of the diodes states will induce a variation in the current distribution and thus a phase shift of 180°. The OFF state of the diode (red diode) is equivalent to a capacitor $C_{off} = 0.042$ pF in parallel with a resistor $R_{OFF} = 300$ kΩ. Whereas the ON state of the diode (green diode), is equivalent to an inductor $L_{ON} = 0.05$ nH in series with a resistor $R_{ON} = 4.2$ Ω. This 1-bit unit cell has been simulated for its two phase states using the commercial software Ansys HFSS with periodic boundary conditions on the unit-cell lateral faces and a Floquet port excitation in normal incidence (Fig. 4). The unit cell presents a phase difference of almost 180°± 20° and a reflection coefficient magnitude smaller than 1.5 dB over the frequency band for both unit cell states, reported in Fig. 4.
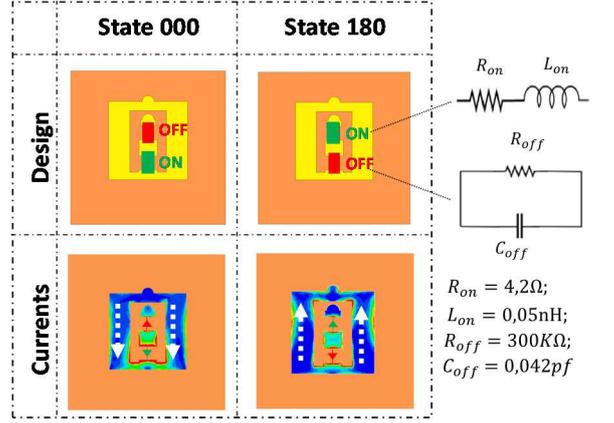

Fig. 3. The two states of the unit cell with the corresponding diode states and current distributions.

III. RECONFIGURABLE REFLECTARRAY: MODELLING, SYNTHESIS AND SIMULATION RESULTS

A. Reflectarray Configuration and Modeling

Previously a hybrid full wave methodology based on analytic expression and full-wave simulations was developed to synthetize, and optimize Transmitting-RIS (transmitarray). It was validated with the measurement results up to 330 GHz in [12], [13] and [14]. This tool has been extended to consider Reflecting-RIS and RA antenna arrays. In this section, the model will be presented briefly. The input data in the model are the following: the focal source radiation pattern, the unit-cells scattering matrix, and their radiation patterns. The data could be considered as ideal cases (ideal unit cell and ideal source) or could be extracted from full-wave simulations (such as HFSS simulation). The structure in Fig. 1 is considered with a RIS of M×M elements. The RA is illuminated by a focal source at a focal distance F. The input power on the focal source is P_1. The complex radiation pattern of the focal source is denoted as $H_{FS}(\theta, \phi)$. The radiation pattern in the mth directions is $H_{FS}(\theta_{FS}^m, \phi_{FS}^m)$; the two components of the pattern in the mth unit cell direction are $H_{FS}^{\theta^m}$ and $H_{FS}^{\phi^m}$. The complex radiation pattern of the unit cell is denoted as $H_{uc}(\theta, \phi)$. The radiation pattern in the direction of the focal source is $H_{uc}(\theta_{uc}^m, \phi_{uc}^m)$; the two components of the pattern of the mth unit cell in the direction of the focal source are $H_{uc}^{\theta^m}$ and $H_{uc}^{\phi^m}$. Therefore, the incident wave received by the mth unit cell is calculated by the following formula:

$$a_1^m = \frac{\lambda e^{-\frac{j2\pi R_m}{\lambda}}}{4\pi R_m} \left(H_{FS}^{\theta^m} H_{uc}^{\theta^m} + H_{FS}^{\phi^m} H_{uc}^{\phi^m} \right) \sqrt{P_1}, \qquad (1)$$

where R_m: is the distance between the focal source and the mth unit cell, and λ : is the wavelength.
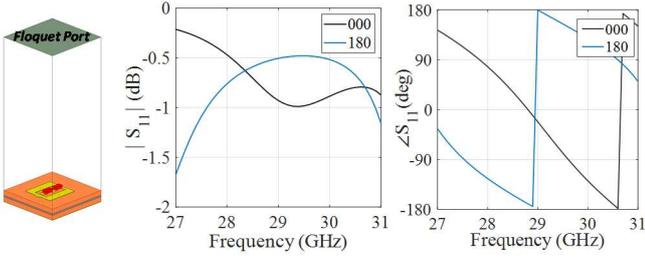
Fig. 4. The unit cell simulation setup , the magnitude and the phase of the reflection coefficients of the two states (State000 and State180).

The reflected wave by the mth unit cell is then calculated using the following formula:

$$b_1^m = S_{11}^m . a_1^m, \qquad (2)$$

where S_{11}^m: is the reflection coefficient of the mth unit cell.

Finally the radiation pattern of the reflectarray (H_{RA}^θ and H_{RA}^ϕ) is computed by the summation of the contribution of each cell, taking into account the reflected wave calculated in equation (2) and the radiation pattern of the unit cell:

$$H_{RA}^{\theta/\phi} = \sum_M b_1^m o \, H_{uc}^{\theta/\phi} \, e^{\frac{j2\pi}{\lambda}(sin\theta cos\phi X_m + sin\theta sin\phi Y_m)}, \quad (3)$$

where X_m and Y_m: are the Cartesian coordinates of the unit cell (in the plane z = 0 , since the RA is placed in the place xoy (Fig. 1)).

The Matlab tool can ensure a full analytical study. Several sweeps could be performed such as: frequency sweep, focal distance sweep, etc… These sweeps help in the optimization of the RA antenna. In Fig. 5, an example of 20×20 unit cells RA is shown. The analytical results calculated in the developed tool are shown in Fig. 5 and in Fig. 6. The different phase distributions for the steering angles [-60°:5°:60°] are calculated as well as the 2D radiation patterns in the plane ϕ = 0° at 29GHz. The 3D radiation pattern for a reflection towards 30° is shown. There are other far-field results that could be extracted from the tool such as other cut planes, the gain vs the frequency, the efficiency etc…

B. Synthesis and Simulation of 4λ×4λ Reflectarray

In order validate the model of the proposed Matlab tool in one hand and to demonstrate the reliability of the designed reconfigurable unit cell in the other hand, a 8×8 unit cell (4λ×4λ, 40.8×40.8mm²) RA is considered. The RA is illuminated using a standard 10-dBi horn placed at a focal distance F =32 mm (F/D = 0.8). For the sake of simplicity, the horn is placed at the middle of the RA. Since the horn is
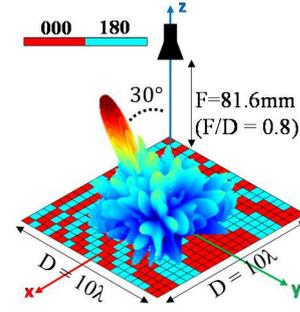

Fig. 5. The adopted scenario in the Matlab Simulation of a RA of 20×20 unit cells and the 3D gain pattern in 30° direction.
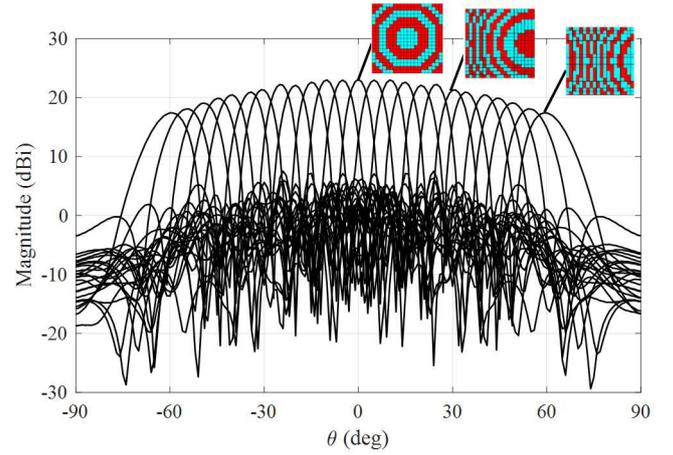

Fig. 6. The gain patterns for different steering angles are calculated analytically in the Matlab tool for a RA of 20×20 unit cells.

covering an angle of the reflection plane (see the 3D sketch of the scenario in Fig. 5) thus, the reflection in broadside is not considered in order to avoid the shadowing caused by the horn. The phase distributions for two steering angles are generated: i) Reflection towards 10°, ii) Reflection towards 30°. The full RA considering the two phase distributions is then simulated in HFSS (Fig. 7) with the Finite Element Boundary Integral (FE-BI) solver.

The simulation results are then compared to the MATLAB theoretical results. In Fig. 8, the pattern for the two reflection cases (10° and 30°) are shown with the corresponding phase distribution. The plots show good agreement between the full-wave simulations and the theoretical results. For the case of the reflection towards 10°, the maximum gain calculated in Matlab is of 15.71dB, and of 14.92 dB the maximum gain exported from HFSS which leads to a small difference of 0.8dB. Whereas in the case of the reflection towards 30°, the gain value is almost the same with a small shift of 1.5° between the two patterns. The side lobes in both cases (10° and 30°) show differences between the analytical and simulation results. This could be explained by the small size of the considered RA. The simulation setup in HFSS (Fig. 7) shows that the size of the horn compared to the size of the RA is too big and this may leads to some coupling effects.
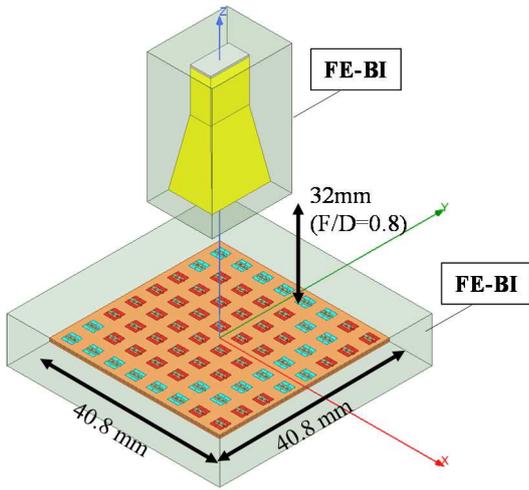
Fig. 7. The HFSS simulation setup of a RA of 8x8 unit cells illuminated in the middle by a standard 10dBi horn.
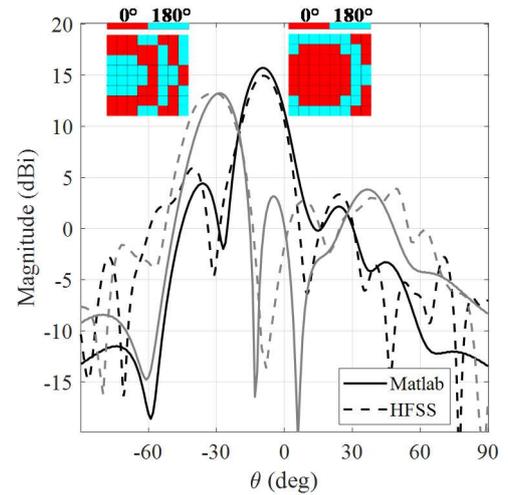

Fig. 8. The 2D gain pattern of the RA of 8x8 unit cells at 29GHz in the plane ϕ=0° for two steering angles -30° and -10°.

In general, the RIS sizes are much bigger than the one considered in this case. The small size was fixed in order to maintain the balance between the validation of the concept and the time consumption of the full-wave simulation. Finally, these patterns demonstrate the feasibility of reconfigurable RA using the developed unit cell.

IV. CONCLUSION

An electronically reconfigurable unit-cell design is proposed in this paper. A 1-bit phase shift is ensured by alternating the states of two p-i-n diodes based on the rotation technique of the current distribution. A 8×8 elements reflectarray is optimized using a developed in-house Matlab tool. The RA is illuminated by a standard horn placed in the middle. The patterns of the full-wave simulation for 10° and 30° pointing demonstrate the feasibility of reconfigurable reflectarray using the designed cell. These results are compared to the analytical ones and show good agreement. The results are very promising in order to extend the code to consider offset illumination. The unit cell will be used to fabricate lager size RA and the measurement results will follow for further validations.

REFERENCES

[1] H. Wymeersch, J. He, B. Denis, A. Clemente, and M. Juntti, "Radio localization and mapping with reconfigurable intelligent surfaces," *IEEE Vehicular Technology Magazine*, vol. 15, no. 4, pp. 52-61, Dec. 2020.

[2] E. Calvanese-Strinati, G. C. Alexandropoulos, H. Wymeersch, B. Denis, V. Sciancalepore, R. D'Errico, A. Clemente, D.-T. Phan-Huy, E. De Carvalho, and P. Popovski, "Reconfigurable, intelligent and sustainable environments for 6G," *IEEE Communications Mag.,* vol. 59, no. 10, pp. 99-105, Oct. 2021.

[3] J. R. Reis, M. Vala, and R. F. S. Caldeirinha, "Review paper on transmitarray antennas," *IEEE Access*, vol. 7, pp. 94171-94188, 2019.

[4] M. H. Dahri, M. I. Abbasi, M. H. Jamaluddin and M. R. Kamarudin, "A review of high gain and high efficiency reflectarrays for 5G communications," *IEEE Access*, vol. 6, pp. 5973-5985, 2018.

[5] M. M. Tahseen, T. A. Denidni, and A. A. Kishk, "Proof of concept low-loss reconfigurable reflectarray for beam steering," *18th Int. Symp. Antenna Tech.and Applied Electromagnetics (ANTEM)*, pp. 1-2, 2018.

[6] J. Perruisseau-Carrier and A. K. Skrivervik, "Monolithic MEMS-based reflectarray cell digitally reconfigurable over a 360° phase range," *IEEE Antennas Wireless Propag. Let.*, vol. 7, pp. 138-141, 2008.

[7] Z. Wang *et al.*, "1 Bit Electronically Reconfigurable Folded Reflectarray Antenna Based on p-i-n Diodes for Wide-Angle Beam-Scanning Applications," in *IEEE Trans. Antennas Propag*, vol. 68, no. 9, pp. 6806-6810, Sept. 2020.

[8] J. Wang and Y. Rahmat-Samii, "Development of novel K-band beam steerable reflectarray for CubeSat internet of space," *IEEE Int. Symp. Antennas Propag. (APS/URSI)*, July 2020.

[9] Q. T. Tran and B. D. Nguyen, "1-bit reflectarray element based on a single switch for reconfigurable reflectarrays," *Antennas Design and Measurement Int. Conf. (ADMInC)*, pp. 142-145,2019.

[10] J. -B. Gros, V. Popov, M. A. Odit, V. Lenets and G. Lerosey, "A reconfigurable intelligent surface at mmWave based on a binary phase tunable metasurface," *IEEE Open Journal Comm. Society*, vol. 2, pp. 1055-1064, 2021.

[11] D. Martinez-de-Rioja, R. Florencio, J. A. Encinar, E. Carrasco and R. R. Boix, "Dual-frequency reflectarray cell to provide opposite phase shift in dual circular polarization with application in multibeam satellite antennas," *IEEE Antennas Wireless Propag. Lett.*, vol. 18, no. 8, pp. 1591-1595, Aug. 2019.

[12] H. Kaouach, L. Dussopt, J. Lanteri, T. Koleck and R. Sauleau, "Wideband low-loss linear and circular polarization transmit-arrays in V-band," *IEEE Trans. Antennas Propag*, vol. 59, no. 7, pp. 2513-2523, July 2011.

[13] A. Clemente, L. Dussopt, R. Sauleau, P. Potier and P. Pouliguen, "Focal distance reduction of transmit-array antennas using multiple feeds," *IEEE Antennas Wireless Propag. Lett.*, vol. 11, pp. 1311-1314, 2012.

[14] O. Koutsos, F. F. Manzillo, A. Clemente and R. Sauleau, "Analysis, rigorous design, and characterization of a three-layer anisotropic transmitarray at 300 GHz," in *IEEE Trans. Antennas Propag*, vol. 70, no. 7, pp. 5437-5446, July 2022.